Catalysis Today 158 (2010) 324–328

Contents lists available at ScienceDirect

Catalysis Today

journal homepage: www.elsevier.com/locate/cattod

The action of Pt in bimetallic Au–Pt/CeO_2 catalyst for water–gas shift reaction

Qiangqiang Yu, Wei Chen, Yang Li, Mingshan Jin, Zhanghuai Suo*

Institute of Applied Catalysis, Yantai University, Yantai 264005, PR China

ARTICLE INFO

Article history:
Available online 10 May 2010

Keywords:
Ceria
Gold
Platinum
Bimetallic catalyst
Water–gas shift reaction

ABSTRACT

Bimetallic Au–M (M = Ni, Cu, Ag, Pt, and Pd) catalysts supported on CeO_2 were prepared by step-by-step impregnation method for water–gas shift reaction. Among them Au–Pt/CeO_2 catalyst shows the highest activity with 78% conversion of CO at 250 °C. The action of platinum in Au–Pt/CeO_2 catalyst was investigated by means of X-ray diffraction, hydrogen temperature-programmed reduction, UV–vis diffuse reflection spectroscopy, and X-ray photoelectron spectroscopy. It is found that the introduction of platinum in Au–Pt/CeO_2 catalyst is responsible for the formation of partly oxidized gold species probably due to the interatomic charge transfer from Au 5d to Pt 5d band. The presence of both gold and platinum is beneficial to the reduction of ceria to Ce^{3+} species as well as the creation of oxygen vacancies and makes the average size of ceria smaller.

1. Introduction

The water–gas shift (WGS) reaction is one of the most attractive reactions, because it can convert carbon monoxide with water vapor to carbon dioxide and hydrogen and provide a pathway for the removal of carbon monoxide and the production of pure hydrogen that can be employed for ammonia synthesis, fuel cells, and other industrial applications [1,2]. Commercial iron–chromium oxides and copper–zinc–aluminum oxides are available for WGS reaction catalysts. However, the working temperatures of these catalysts are higher than the temperature in fuel cell and they are not ideal candidates for the application. In recent years, rapidly accelerating interests have been focused on gold nanoparticles supported on various oxides as they shows high activities and stability in low-temperature CO oxidation, WGS reaction, liquid selective oxidation of organic compounds, and many other reactions [3–11]. It has been well known that support plays a critical role in dispersing nanosized gold active components and determining its catalytic activity [2,3,12,13]. Ceria has facile Ce^{4+}/Ce^{3+} redox performance and good oxygen storage capacity. Andreeva et al. [14] and Fu et al. [15] reported that gold catalyst supported on ceria gave good activity and stability for WGS reaction.

Some studies [16–18] indicate that adding second active metal to gold catalyst can markedly change the chemical state of active gold species and promote its catalytic activity in WGS reaction. Further the second metal can also stabilize gold nanoparticles and prohibit from sintering active gold species. Venugopal et al. [16] found that owing to the strong interaction between Pd and Au, Au particles became smaller and the activity of gold catalyst was obviously improved. In previous works, we prepared Au–Pd/SiO_2 [19], Au–Pd/Al_2O_3 [20] and Au–Ni/SiO_2 [21] catalysts and concluded that there was evident interaction between gold and palladium or nickel. Here we prepared the bimetallic Au–M/CeO_2 (M = Ni, Cu, Ag, Pt, and Pd) catalysts for WGS reaction. Attention was paid to the action of platinum in Au–Pt/CeO_2 catalyst by mean of X-ray diffraction (XRD), hydrogen temperature-programmed reduction (H_2-TPR), UV–vis diffuse reflection spectroscopy (UV–vis DRS), and X-ray photoelectron spectroscopy (XPS) characterization.

2. Experimental

2.1. Catalyst preparation

Ceria support was prepared by precipitation method. An aqueous solution of cerium nitrate was precipitated to hydroxide with ammonia at vigorous stir. The resulting slurry precipitate went through filtering, washing repeatedly with deionized water, drying at 120 °C for 12 h. After calcining the solid sample in air at 400 °C for 5 h, yellow ceria was obtained.

The monometallic Au/CeO_2 or M/CeO_2 (M = Ni, Cu, Ag, Pt, and Pd) catalyst was prepared through impregnating ceria support with an amount of relevant metal salt solution and then washing, drying, and calcining. To prepare Au–M/CeO_2 catalyst, the M/CeO_2 was impregnated overnight with chloroauric acid solution. The dried sample was followed by calcination in air at 400 °C for 4 h and obtained Au–M/CeO_2 catalyst. The Au–Pt/CeO_2 catalysts were also prepared using different impregnation procedures. For example, Au-promoted Pt/CeO_2 was prepared by impregnat-

* Corresponding author at: Institute of Applied Catalysis, Yantai University, 32 Qingquan Road, Yantai, PR China. Tel.: +86 0535 6902514; fax: +86 0535 6902233.
E-mail address: ytzhsuo@sina.com (Z. Suo).

0920-5861/$ – see front matter © 2010 Elsevier B.V. All rights reserved.
doi:10.1016/j.cattod.2010.04.005

ing Pt/CeO_2 with chloroauric acid solution, denoted as $Au–Pt/CeO_2$, and Pt-promoted Au/CeO_2 was prepared by impregnating Au/CeO_2 with chloroplatinic acid solution, denoted as $Pt–Au/CeO_2$, and Au- and Pt-promoted CeO_2 was prepared by impregnating CeO_2 with the mixture solution of chloroauric acid and chloroplatinic acid, denoted as $Au(Pt)/CeO_2$. The total metal content maintains at 2 wt% and Au/M mole ratio in $Au–M/CeO_2$ is 1.

2.2. Catalyst characterization

X-ray powder diffraction (XRD) measurements were performed on an XRD-6100 powder diffractometer (Shimadzu Analytical Instrument Co., Japan) employing Cu Kα radiation. The diffraction patterns were recorded in a scan rate of 6°/min with 0.02° data interval.

Hydrogen temperature-programmed reduction (H_2-TPR) measurements were carried out on a TP-5000 apparatus (Tianjin Xianquan Adsorption Instrument Ltd Co., China). The sample in a quartz tube was first pre-treated with 20 ml/min of nitrogen for 30 min at 120 °C and then reduced in a mixture gas of 10% hydrogen and 90% argon (flow rate 20 ml/min) at elevating temperature from room temperature up to 800 °C at a rate of 10 °C/min. The consumption of hydrogen over the sample was monitored by a thermal conductivity detector.

UV–vis diffuse reflectance spectroscopy (UV–vis DRS) was recorded using a TU-1901 (Beijing General Analytical Instrument Ltd Co., China) with $BaSO_4$ as the internal standard. The scanning patterns were recorded at 200–800 nm in a step-scan mode with a step of 5 nm.

X-ray photoelectron spectroscopy (XPS) was recorded on a VG ESCALAB-210 spectrometer using Mg Kα radiation (1253.6 eV) at 200 W. All binding energies were adjusted to the C 1s peaks at 285.0 eV. All measurements were carried out at room temperature and at below 2.7×10^{-6} Pa pressure.

2.3. Catalytic activity measurements

The catalytic performance of bimetallic $Au–M/CeO_2$ catalyst for WGS reaction was evaluated in a fixed-bed flow reactor at atmospheric pressure. The following conditions were applied: 0.5 cm^3 of catalyst, 10 ml/min of CO, 31.1 kPa of water vapor. The content of CO, CO_2, and H_2 were analyzed by on-line gas chromatography with FID detector and a graphitized carbon black column. A QIC-20 quadruple mass spectrometer (Hiden Analytical Ltd., UK) was also used to gas detection. The catalytic activity was expressed as CO conversion calculated by H_2 amount in outlet mixture.

3. Results and discussion

3.1. WGS reaction activity

The WGS reaction activities over bimetallic $Au–M/CeO_2$ (M = Ni, Cu, Ag, Pt, and Pd) catalysts were evaluated and the results are shown in Fig. 1a. The activity is found to be as function of reaction temperature for all the catalysts studied. And different catalyst shows very different catalytic activity. For example, the $Au–Pt/CeO_2$ catalyst displays a higher activity than other catalysts. The WGS reaction activities over these catalysts decrease as the following order: $Au–Pt/CeO_2 > Au–Ni/CeO_2 > Au/CeO_2 > Au–Cu/CeO_2 > Au–Ag/CeO_2 > Au–Pd/CeO_2$. Recently, Hurtado-Juan's work also showed $Au–Pt/CeO_2$ had the highest WGS reaction activity [18]. It is very clear that the addition of such as platinum or nickel components brings a positive effect on gold catalysts for WGS reaction.

As shown in Fig. 2, the impregnation procedures of both Au and Pt active component have some effect on catalytic activity of the bimetallic catalyst. Relatively, $Au–Pt/CeO_2$ catalyst exhibits higher activity than $Pt–Au/CeO_2$ or $Au(Pt)/CeO_2$ catalysts. Furthermore, the activity increases obviously with Pt loadings in $Au–Pt/CeO_2$. For example, CO conversion is only 8.9% at 200 °C for Au/CeO_2 catalyst. When the Pt loading reaches 0.5%, 1%, and 2%, CO conversion improves to 37.6%, 46.5% and 54.1%, respectively.

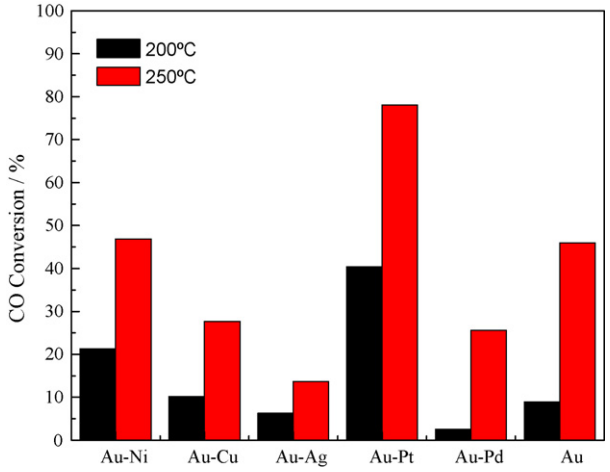

Fig. 1. Water–gas shift reaction activity over Au/CeO_2 and $Au–M/CeO_2$ (M = Ni, Cu, Ag, Pt, and Pd) catalysts at 200 and 250 °C.

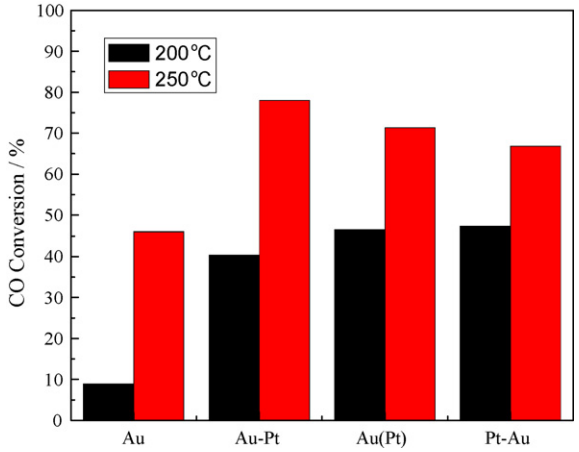

Fig. 2. Water–gas shift reaction activity over $Au–Pt/CeO_2$ catalysts prepared by different impregnation sequence at 200 and 250 °C.

3.2. XRD patterns

Fig. 3 represents the XRD patterns of bimetallic $Au–M/CeO_2$ (M = Cu, Ni, Ag, Pd, and Pt) catalysts. In the XRD patterns of all samples, the diffraction lines of Au, Pt or Au_xPt_y alloy phases are not visible and the diffraction lines of ceria are typical of the cubic crystal structure of fluorite type oxide. The fact that the interplanar crystal space $d(1\,1\,1)$ of all studied samples are higher than that of stoichiometric ceria indicates that the addition of Au and M has an effect on the structure of ceria, resulting in the creation of oxygen vacancies and Ce^{3+} species [22]. Moreover, the introduction of Au and M to ceria makes the size of ceria smaller. According to Scherrer's equation, the average size of ceria particles is 132.4 nm for pure CeO_2; 103.5 nm for $Au–Cu/CeO_2$; 102.3 nm for $Au–Ni/CeO_2$; 101.1 nm for $Au–Ag/CeO_2$; 109.1 nm for $Au–Pd/CeO_2$; and 96.9 nm for $Au–Pt/CeO_2$. The size of ceria particles is an important factor controlling WGS reaction activity.

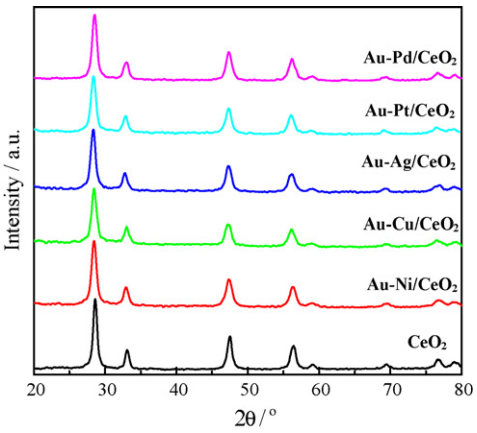

Fig. 3. XRD patterns of CeO_2 and Au–M/CeO_2 (M = Ni, Cu, Ag, Pt, and Pd) bimetallic catalysts.

3.3. H_2-TPR analysis

Ceria is capable of being readily reduced and reoxidized, so H_2-TPR is employed to study the reducibility of ceria-based catalysts. Fig. 4 shows TPR profiles of CeO_2, Au/CeO_2, Pt/CeO_2, and Au–Pt/CeO_2 samples. The TPR profile of pure CeO_2 consists of a low-temperature reduction peak at T_{max} = 475 °C and a high-temperature reduction peak at T_{max} = 790 °C. The former is assigned to the reduction of surface ceria and the later is connected to the reduction of bulk ceria [14]. When gold was supported on CeO_2, the reduction of CeO_2 remains unchanged but there appears a new reduction peak at T_{max} = 175 °C which could be related to the reduction of oxygen species on the fine gold particles [2]. In Pt/CeO_2, the high-temperature reduction peak shifts significantly to the lower temperature at T_{max} = 720 °C, indicating that the reduction of surface ceria can be enhanced by Pt. And moreover, there is an overlap between the reduction of the Pt^{2+} and the reduction of the surface ceria oxygen species. For bimetallic Au–Pt/CeO_2 catalyst, the reduction of oxygen species on the fine gold particles emerges at 145 °C and the low-temperature reduction peak of ceria is shifted to at T_{max} = 390 °C. These results indicated that the coexistence of both Au and Pt is beneficial to the reduction of oxygen species on the fine gold particles and the reduction of surface ceria.

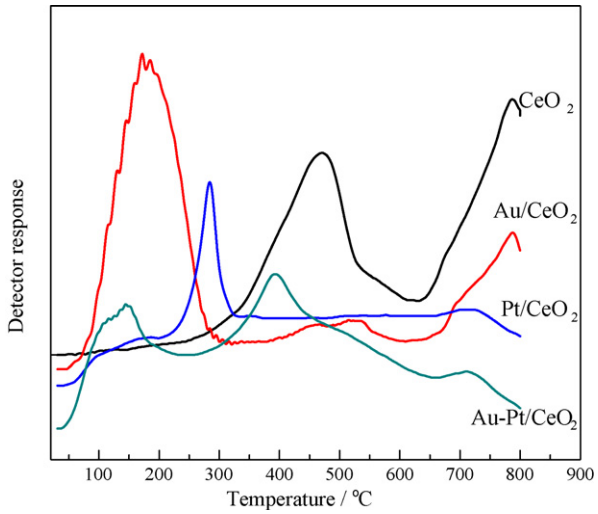

Fig. 4. TPR profiles of CeO_2, Au/CeO_2, Pt/CeO_2, and Au–Pt/CeO_2 samples.

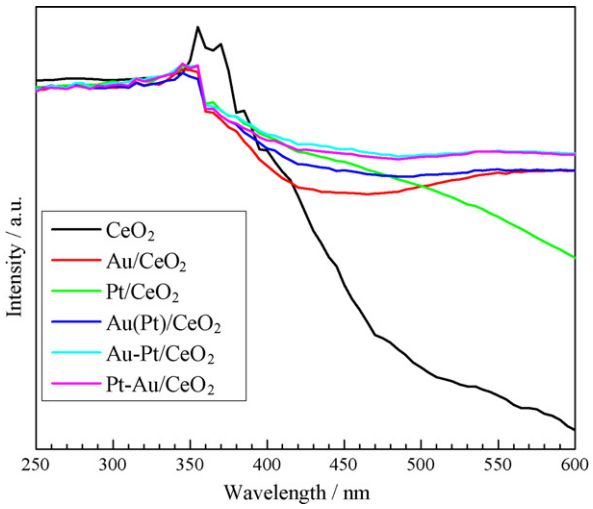

Fig. 5. UV–vis diffuse reflection spectra of CeO_2, Au/CeO_2, Au–Pt/CeO_2, Au(Pt)/CeO_2, Pt–Au/CeO_2, and Pt/CeO_2 samples.

3.4. UV–vis DRS analysis

Fig. 5 shows UV–vis diffuse reflection spectra of CeO_2, Au/CeO_2, Pt/CeO_2, Au–Pt/CeO_2, Au(Pt)/CeO_2, and Pt–Au/CeO_2 samples. Ceria possesses two characteristic bands centered at 355 and 370 nm, assigned to the charge transfer band of ceria ($Ce_{4f} \leftarrow O_{2p}$). After doping Au to ceria, the two bands disappear and a new band centered at about 450 nm is observed. The band is assigned to the typical plasmon resonance absorption of gold nanoparticles [23]. For Pt/CeO_2 catalyst, the present of Pt also makes the two bands of ceria disappearance. We do not observe the absorption peak of Pt in UV region. Au–Pt/CeO_2, Au(Pt)/CeO_2, and Pt–Au/CeO_2 catalysts give very similar spectra as Au/CeO_2. Due to the presence of Pt, however, the intensity of Au absorption band enhances distinctly. It suggests that the addition of Pt promotes the reduction of Au^{3+} and the production of Au particles.

3.5. XPS analysis

XPS is used to investigate the interaction between gold and platinum in gold–platinum catalysts supported on ceria. The XPS spectra of Au 4f, Pt 3d, Ce 3d, and O 1s for the corresponding samples are shown in Figs. 6–9, respectively, and the derived XPS data are summarized in Table 1. It can be seen from Fig. 6 that the Au $4f_{7/2}$ peak is centered at 84.0, 84.1 and 84.3 eV for Au/CeO_2, for Au–Pt/CeO_2 and for Au(Pt)/CeO_2, respectively. According to the reports of Chastain [24], the Au $4f_{7/2}$ peaks of Au^0, Au^+, and Au^{3+} appear at 83.8, 86.2, and 87.3 eV, respectively. So it can be certain that most of gold in these catalysts is metallic, but part of gold remains ionic. Moreover, the presence of Pt can achieve a strong metal-support interaction to stabilize gold ions. While metallic gold on ceria surface decreases, ionic gold component increases with the platinum content in the samples. This result is in agreement with the higher active Au(Pt)/CeO_2 and Au–Pt/CeO_2 catalysts.

Two peaks due to Pt $4f_{7/2}$ and Pt $4f_{5/2}$ transitions are detected in Pt/CeO_2, Au–Pt/CeO_2, and Au(Pt)/CeO_2 samples, as shown by Fig. 7. According to the literature [25,26], the Pt $4f_{7/2}$ peak at 71.0 eV and the Pt $4f_{5/2}$ peak at 74.2 eV are assigned to Pt metal; the peaks at 71.9 and 75.1 eV are Pt^{2+} species and the peaks at 74.3 and 77.5 eV are Pt^{4+} species. In three samples studied here, the Pt $4f_{7/2}$ and Pt $4f_{5/2}$ peaks appear at 73.48, 76.65 eV for Pt/CeO_2; 73.25, 76.32 eV for Au–Pt/CeO_2; and 73.63, 76.62 eV for Au(Pt)/CeO_2, respectively, shifting markedly to higher energy region. This indicates that platinum is in +4 state in the calcination process of these samples.

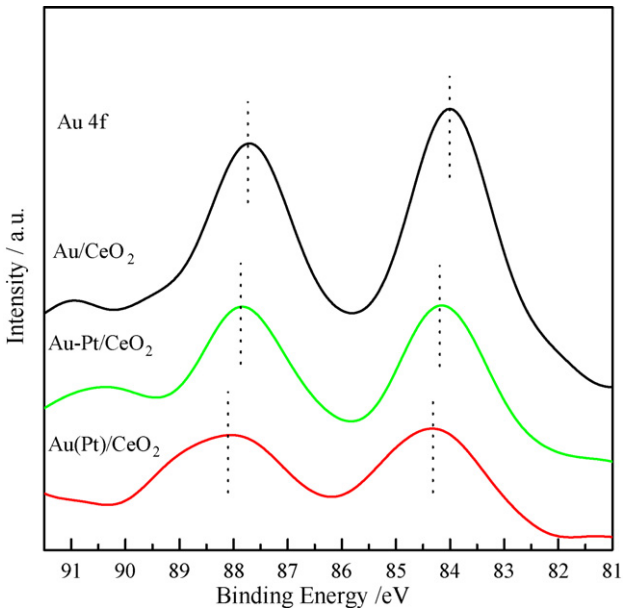

Fig. 6. Au 4f XPS spectra of Au/CeO_2, $Au–Pt/CeO_2$, and $Au(Pt)/CeO_2$ samples.

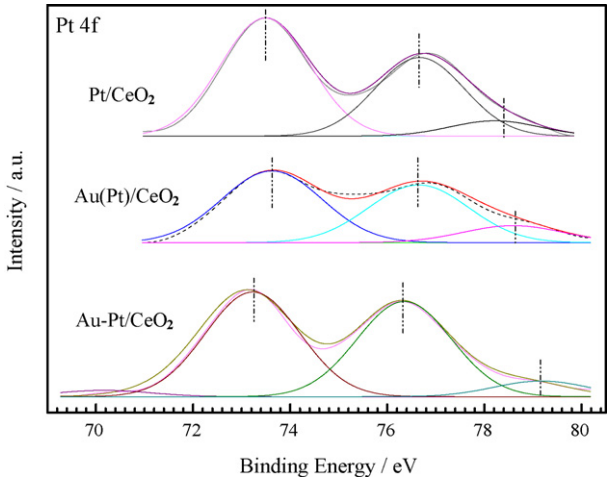

Fig. 7. Pt 4f XPS spectra of Pt/CeO_2, $Au(Pt)/CeO_2$, and $Au–Pt/CeO_2$ samples.

The XPS spectra of Ce 3d core electron levels of Au/CeO_2, $Au(Pt)/CeO_2$, $Au–Pt/CeO_2$, and Pt/CeO_2 samples are illustrated in Fig. 8. The signal of the 3d level has a very complicated structure. The Ce 3d XPS spectra are fitting according to eight peaks [27,28], denoted as two groups (U, U^I, U^{II}, U^{III} and V, V^I, V^{II}, V^{III}).

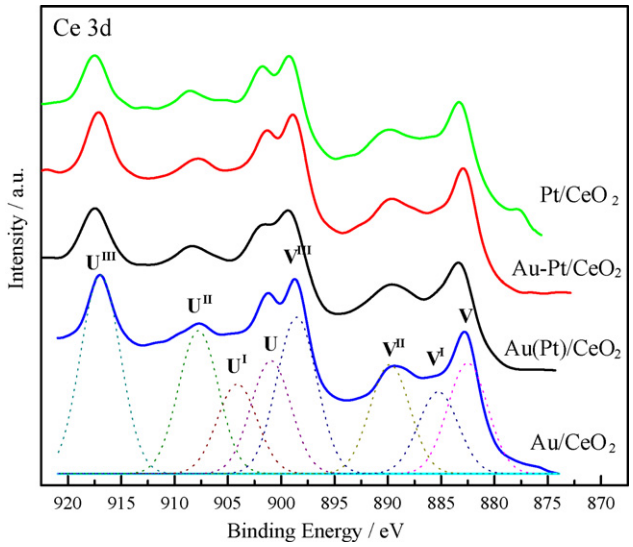

Fig. 8. Ce 3d XPS spectra of Au/CeO_2, $Au(Pt)/CeO_2$, $Au–Pt/CeO_2$, and Pt/CeO_2 samples.

The peaks of U, U^{II}, U^{III} and V, V^{II}, V^{III} refer to Ce(IV) $3d_{3/2}$ and $3d_{5/2}$, respectively, while both U^I and V^I stand for Ce(III) $3d_{3/2}$ and $3d_{5/2}$, respectively. The Ce 3d spectra for all the catalysts are similar to pure CeO_2 spectra, showing well resolved Ce(IV) lines. The 3d level is formed by two series peaks: one is $3d_{5/2}$ (882.54 eV) with two very pronounced "shake-up" satellites (889.88 and 898.54 eV) and

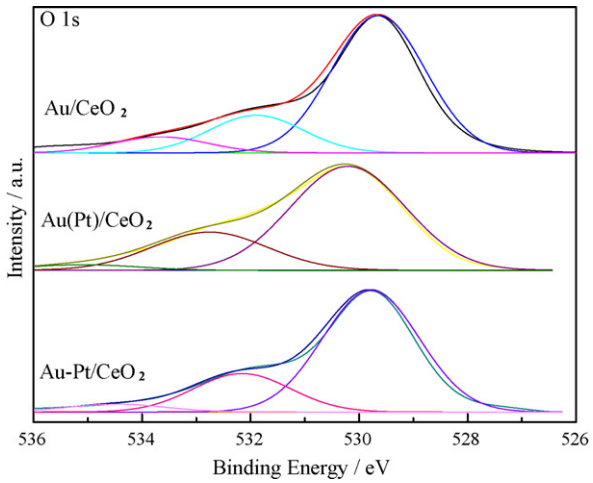

Fig. 9. O 1s XPS spectra of Au/CeO_2, $Au(Pt)/CeO_2$, and $Au–Pt/CeO_2$ samples.

Table 1
The binding energy of Au 4f, Pt 4f, Ce 3d, and O 1s from XPS of all studied catalysts.

Catalysts	Au 4f		Pt 4f		Ce 3d		O 1s	
	$4f_{7/2}$ (eV)	$4f_{5/2}$ (eV)	$4f_{7/2}$ (eV)	$4f_{5/2}$ (eV)	$3d_{5/2}$ (eV)	$3d_{3/2}$ (eV)	BE (eV)	At (%)
Au/CeO_2	84.01	87.70	73.48[a]	76.65[a]	V 882.54 V^I 885.30 V^{II} 889.88 V^{III} 898.54	U 900.99 U^I 904.04 U^{II} 907.81 U^{III} 916.98	529.60 531.85 533.74 530.21	75.78
$Au(Pt)/CeO_2$	84.32	88.13	73.63	76.62	883.36	901.80	532.70 535.21 529.78	80.76
$Au–Pt/CeO_2$	84.14	87.87	73.25	76.32	882.95	901.29	532.20 534.47	76.22

[a] Pt $4f_{7/2}$ and Pt $4f_{5/2}$ in Pt/CeO_2 sample.

another is $3d_{3/2}$ (900.99 eV) with the same characteristics (907.81 and 916.98 eV). It should be noted that pure ceria always contains a small percentage of Ce(III) oxide characterized by the presence of peaks, indicated by U^I (904.04 eV) and V^I (885.30 eV), attributed to the Ce $3d_{3/2}$ and Ce $3d_{5/2}$ components of Ce(III) [29]. The presence of Ce(III) implies the defect structure CeO_{2-x} due to oxygen vacancies. This transformation of Ce(IV) to Ce(III) driven by oxygen vacancies may be the key to understanding the catalytic properties of ceria. It has to be mentioned that the addition of Pt could make Ce(III) components decrease.

XPS spectra of O 1s region of Au/CeO_2, $Au(Pt)/CeO_2$, and $Au–Pt/CeO_2$ are shown in Fig. 9. The O 1s peak of Au/CeO_2 was fitted with three components (Table 1): the first at about 529.60 eV is typical of the lattice oxygen of CeO_2, the second at about 531.85 eV is typical of hydroxide species and the third at 533.74 eV is due to the presence of Ce^{3+} surface defects [30]. The binding energies of the three peaks shift to higher region due to the presence of platinum, which could be connected with the lower degree of Ce^{3+} surface defects. Guzman et al. [31] reported that nanocrystalline CeO_2 could supply reactive oxygen in the form of surface superoxide species and peroxide adspecies at the one-electron defect site to the supported active species of gold for the oxidation of CO. This result is in a good agreement with our results. Besides, the concentration of the surface oxygen of ceria obviously increases in the presence of Pt. It causes the formation of oxygen vacancies, located mainly on the catalyst surface. This is why the bimetallic Au and Pt catalysts possess the higher WGS reaction activity than monometallic Au/CeO_2 or Pt/CeO_2 catalyst.

Andreeva et al. [2,14,22] suggested that on reduced samples nanosized metallic gold clusters are present in contact with oxygen-vacancy defects on ceria surface and that these are responsible for high catalytic activity in WGS reaction. The results from Flytzani-Stephanopoulos' group documented the importance of the interaction between gold and the oxygen of ceria by showing that only the gold species embedded or otherwise associated with ceria [Au_n–O–Ce] are the active sites for WGS reaction [15,26,32,33]. The number of these gold species supported on ceria increases with decreasing the crystal size of ceria. Similarly, oxidized clusters of platinum bound to ceria, [Pt_n–O–Ce], were found and all the platinum had diffused in the subsurface layers of ceria. While the presence of metallic platinum and gold nanoparticles on ceria causes a dramatic reducibility enhancement of the surface oxygen of ceria, the oxidized species of Au and Pt strongly bound to ceria are less reducible.

For Au-based bimetallic catalyst, Lee et al. [34] and Sarkany et al. [35] suggested that the increase in Pd d-band electron density for Au–Pd bimetallic particles originates from the charge transfer from the Au $5d^{10}$ to Pd d-band. Our previous works on $Au–Pd/SiO_2$ [19] and $Au–Pd/Al_2O_3$ [20] catalysts indicated that the presence of gold atoms affected the electrons redistribution in Pd d-band and the redistribution transferred from the electrons on gold atoms to palladium atoms and formed partially oxidized gold species. Recently Bus and van Bokhoven [36] investigated electronic and geometric structure of Au–Pt bimetallic particles using XPS, EXAFS and XANES techniques and found that the Pt L_3 edge shifted to higher energy and the Au L_3 edge shifted to lower energy. These changes are considered as the interatomic charge transfer from Au 5d to Pt 5d band, accompanied by intraatomic charge redistributions. These coincide with our characterization results in that the introduction of platinum can improve the formation of ionic gold species.

4. Conclusions

Structural and catalytic properties in low-temperature WGS reaction have been investigated for bimetallic $Au–M/CeO_2$ (M = Cu, Ni, Ag, Pd, and Pt) catalysts. The addition of metal M has an influence on catalytic activity due to the nature of modifier metal. The components such as platinum and nickel exert an advance effect on catalysis by metals for WGSR. The bimetallic $Au–Pt/CeO_2$ catalyst shows higher WGS reaction activities compared to the other systems. The introduction of gold or platinum active component not only makes the size of CeO_2 smaller and but also affects the structure of CeO_2, resulting in the creation of oxygen vacancies and Ce^{3+} ions. Furthermore, the addition of Pt is conducive to the formation of $Au^{\delta+}$ because of the interatomic charge transfer from Au 5d to Pt 5d band, accompanied by intraatomic charge redistributions. The presence of both metallic and ionic gold species, the high concentration of surface oxygen as well as the low degree of Ce^{3+} surface defects determine simultaneously the WGS reaction activity of the bimetallic Au–Pt catalyst.

Acknowledgements

The Project is sponsored by National Natural Science Foundation of China (No. 20473070 and 20973148). Assistance in the XPS measurement by Ms Gao Ling of Lanzhou Institute of Chemical Physics, Chinese Academy of Sciences, is kindly acknowledged.

References

[1] R. Burch, Phys. Chem. Chem. Phys. 8 (2006) 5483.
[2] D. Andreeva, Gold Bull. 35 (2002) 82.
[3] M. Haruta, N. Yamada, T. Kobayashi, S. Iijima, J. Catal. 115 (1989) 301.
[4] S. Carrettin, P. Concepción, A. Corma, J.M.L. Nieto, V.F. Puntes, Angew. Chem. Int. Ed. 43 (2004) 2538.
[5] D. Andreeva, V. Idakiev, T. Tabakova, A. Andreev, R. Giovanoli, Appl. Catal. A: Gen. 135 (1996) 275.
[6] N. Thielecke, K.-D. Vorlop, U. Prüße, Catal. Today 122 (2007) 266.
[7] Z.-R. Tang, J.K. Edwards, J.K. Bartley, S.H. Taylor, A.F. Carley, A.A. Herzing, C.J. Kiely, G.J. Hutchings, J. Catal. 249 (2007) 208.
[8] D.I. Enache, J.K. Edwards, P. Landon, B. Solsona-Espriu, A.F. Carley, A.A. Herzing, M. Watanabe, C.J. Kiely, D.W. Knight, G.J. Hutchings, Science 311 (2006) 362.
[9] A. Corma, P. Serna, Science 313 (2006) 332.
[10] A. Venezia, R. Murania, G. Pantaleo, G. Deganello, Gold Bull. 40 (2007) 130.
[11] M.O. Nutt, K.N. Heck, P. Alvarez, M.S. Wong, Appl. Catal. B: Environ. 69 (2006) 115.
[12] G.C. Bond, D.T. Thompson, Catal. Rev. Sci. Eng. 41 (1999) 319.
[13] M.B. Cortie, E. van der Lingen, Mater. Forum 26 (2002) 1.
[14] D. Andreeva, V. Idakiev, T. Tabakova, L. Ilieva, P. Falaras, A. Bourlinos, A. Travlos, Catal. Today 72 (2002) 51.
[15] Q. Fu, S. Kudriavtseva, H. Saltsburg, M. Flytzani-Stephanopoulos, Chem. Eng. J. 93 (2003) 41.
[16] A. Venugopal, J. Aluha, M.S. Scurrell, Catal. Lett. 90 (2003) 1.
[17] V. Idakiev, T. Tabakova, A. Naydenov, Z.-Y. Yuan, B.-L. Su, Appl. Catal. B: Environ. 63 (2006) 178.
[18] M.-A. Hurtado-Juan, C.M.Y. Yeung, S.C. Tsang, Catal. Commun. 9 (2008) 1551.
[19] C. Ma, X. Li, M. Jin, W. Liao, R. Guan, Z. Suo, Chin. J. Catal. 28 (2007) 535.
[20] Z. Suo, C. Ma, M. Jin, T. He, L. An, Catal. Commun. 9 (2008) 2187.
[21] Z. Suo, A. Lv, H. Lv, M. Jin, T. He, Catal. Commun. 10 (2009) 1174.
[22] D. Andreeva, I. Ivanov, L. Ilieva, J.W. Sobczak, G. Avdeev, K. Petrov, Top. Catal. 44 (2007) 173.
[23] M. Daniel, D. Astruc, Chem. Rev. 104 (2004) 293.
[24] J. Chastain, Handbook of X-ray Photoelectron Spectroscopy, Perkin-Elmer Corp., Eden Prairie, MN, 1992.
[25] P. Bera, K.R. Priolkar, A. Gayen, P.R. Sarode, M.S. Hegde, S. Emura, R. Kumashiro, V. Jayaram, G.N. Subbanna, Chem. Mater. 15 (2003) 2049.
[26] D. Pierre, W. Deng, M. Flytzani-Stephanopoulos, Top. Catal. 46 (2007) 363.
[27] M. Alifanti, B. Baps, N. Blangenois, J. Naud, P. Grange, B. Delmon, Chem. Mater. 15 (2003) 395.
[28] M. Romeo, K. Bak, J. El Fallah, F. Le Normand, L. Hilaire, Surf. Interface Anal. 20 (1993) 508.
[29] P. Dutta, S. Pal, M.S. Seehra, Y. Shi, E.M. Eyring, R.D. Ernst, Chem. Mater. 18 (2006) 5144.
[30] D. Andreeva, P. Petrova, J.W. Sobczak, L. Ilieva, M. Abrashev, Appl. Catal. B: Environ. 67 (2006) 237.
[31] J. Guzman, S. Carrettin, A. Corma, J. Am. Chem. Soc. 127 (2005) 3286.
[32] Q. Fu, W. Deng, H. Saltsburg, M. Flytzani-Stephanopoulos, Appl. Catal. B: Environ. 56 (2005) 57.
[33] Q. Fu, H. Saltsburg, M. Flytzani-Stephanopoulos, Science 301 (2003) 935.
[34] A.F. Lee, C.J. Baddeley, C. Hardacre, R.M. Ormerod, R.M. Lambert, G. Schmid, H. West, J. Phys. Chem. B 99 (1995) 6096.
[35] A. Sarkany, P. Hargittai, A. Horvath, Top. Catal. 46 (2007) 121.
[36] E. Bus, J.A. van Bokhoven, J. Phys. Chem. C 111 (2007) 9761.